Integrating VES and 2D ERI for near-surface characterization in a crystalline basement terrain

Ahzegbobor P. Aizebeokhai, Olubukola Ogungbade and Kehinde D. Oyeyemi, Covenant University*

Summary

Geoelectrical resistivity is one of the most common geophysical methods for near-surface characterization in many applications including hydrogeologic, environmental, engineering and mining investigations. This case study integrates vertical electrical sounding (VES) with two-dimensional (2D) electrical resistivity imaging (ERI) to characterize the near-surface in a crystalline basement terrain. The investigation was conducted in Ado-Ekiti, southwestern Nigeria to delineate the basement aquifer by characterizing the weathered and fractured zones of the basement rocks. The study is part of the preliminary assessment of groundwater potential in the area. Dipole-dipole array used for the 2D ERI proved to be effective in detecting weathered and fractured zones in crystalline basement rocks. The integration of VES with 2D ERI enhanced the reliability of the characterization.

Introduction

Groundwater occurrence in basement rocks is mainly due to the development of secondary porosity and permeability resulting from the weathering and fracturing of the crystalline igneous and metamorphic basement rocks. Thus, basement aquifers are usually localized and confined to the weathered and fractured zones of the basement rocks (Carruthers, 1985; Palacky et al., 1981). Geophysical surveys are conducted to characterise the weathering profile and delineate the weathered and fractured zones that forms the localized basement aquifers. Geoelectrical resistivity is one of the oldest and most common geophysical methods widely used for near-surface characterization in hydrologic, environmental and geotechnical investigations (e.g. Aizebeokhai et al., 2016; Kazakis et al., 2016; Loke et al., 2013; Niwas and Celik, 2012; Rucker et al., 2010).

Geoelectrical resistivity techniques, which essentially determine the spatial distribution of subsurface resistivity, have been successful in mapping basement features of hydrologic importance in near-surface characterization. The traditional survey is conducted as vertical electrical sounding (VES) to determine the resistivity variation with depth at a given point with the assumption that the resistivity distribution does not varies laterally. This one-dimensional (1D) variation in subsurface resistivity is used to delineate the lithologic layering; however, it often produce inaccurate and distorted geologic models in complex geologic environments characterised with significant lateral variations in the resistivity distribution (Aizebeokhai et al., 2010; Pous et al., 1996). Two-dimensional (2D) and/or three-dimensional (3D) electrical resistivity imaging (ERI) which produce more realistic models are used to map the resistivity variations in such complex and multi-scale geologic environments.

In groundwater exploration in crystalline basement complex terrain, the weathered and fractured zones characterised with high secondary porosity and permeability that provide preferential flow paths for groundwater in the crystalline basement rocks are commonly sort for. Dipole-dipole array is one of the most sensitive electrode configurations to such basement features (Dahlin and Zhou, 2004; Reiser et al., 2009; Wiwattanchang and Giao, 2011). Thus, dipole-dipole array is suitable for ERI surveys for characterising basement structures. In this study, 2D ERI conducted with dipole-dipole array was integrated with VES to characterize the near-surface in a crystalline basement complex terrain. The regolith and weathered and fractured zones that largely controls the occurrence and flow of groundwater in crystalline basement rocks were delineated. The survey was conducted as part of the preliminary assessment of groundwater potential in Basiri area of Ado-Ekiti, southwestern Nigeria.

Study Area

The study area, located in Basiri, Ado-Ekiti, southwestern Nigeria, is characterised with sparsely distributed hills and knolls; mean elevation is 440 m above mean sea level. The climate is tropical humid marked by distinct dry and rainy seasons that spans between November and March, and April and October respectively. The mean annual rainfall is greater than 2300 mm, and average monthly temperature ranges between 22°C in July and 31°C in February. The area is underlain by crystalline basement rocks of Precambrian age, which are mainly granitic intrusions and highly deformed metamorphic rocks (Figure 1). The dominant rocks are pegmatite, quartz and quartz-schists, biotite granite and undifferentiated gneiss complex (Schist). The weathering of these rocks results in a thick lateritic overburden.

Geoelectrical Resistivity Survey

The survey consists of thirty (30) VESs using Schlumberger array and four (4) 2D ERI traverses using dipole-dipole array (Figure 2). The survey parameters for the ERI are presented in Table 1. The electrode positions for the data measurements were clearly marked and pegged before the commencement of the survey so as to minimize electrodes positioning errors. The ABEM Terrameter (SAS 1000/4000 series) for the data measurements was set for repeat measurement with minimum and maximum stacking of 3 and 6 respectively; the injected current was set to a minimum of 20.0 mA and maximum of 200.0 mA. Effective contact between the electrodes and the ground was ensured during the survey while maintaining good connectivity between the electrodes and the connecting cables was also maintained.

The observed apparent resistivity data sets for the VES were processed using Win-Resist computer program to determine the geoelectric model parameters for the layers delineated. The initial models for the computer iteration were obtained by matching the field curves on bi-logarithmic sheets with theoretical curves. The 2D ERI data sets were inverted using RES2DINV inversion code (Loke, 2008) which uses nonlinear optimization technique to determine the 2D inverse model of the subsurface resistivity distribution (Griffiths and Barker, 1993; Loke and Barker, 1996). The RES2DINV inversion program subdivides the subsurface into series of rectangular blocks based on the electrode array and spread for the survey. Both smoothness constrained least-squares (L_2-norm) and robust (L_1-norm) inversion algorithms were used for the inversion. The smoothness constrained inversion technique is most suitable in areas where the resistivity distribution varies smoothly, while the robust inversion is essentially a blocky optimization useful in areas with resistivity distribution of approximately homogeneous regions separated by sharp boundaries. Smoothness constrained inversion minimizes the difference between the observed and calculated apparent resistivity data set through an iterative process while robust inversion attempts to find resistivity models that minimize the absolute values of the data misfit in a least-squares sense (Loke et al., 2013; Olayinka and Yaramanci, 2000).

Results and Discussions

The weathering profile developed above crystalline basement rocks consists of the regolith and bedrock. The regolith is a product of in-situ chemical weathering of the basement rocks and consists of the collapsed zone (top soil) and saprolite which may be divided into upper and lower units; the bedrock consists of the weathered and fractured basement (saprock), and fresh basement (Acworth, 1987; Wright, 1992). The lithologic units of the basement rocks are identified as distinct geoelectric layers with the collapsed zone and bedrock characterised with high resistivities. The intermediate layer (saprolite) represents decomposed crystalline basement rocks with relatively high porosity; it is commonly saturated with groundwater and is characterised with relatively low resistivity anomaly. Thus, three-layer or four-layer geoelectric models are commonly adopted in interpreting resistivity sounding curves in crystalline basement environments (McDowell, 1979; Olayinka, 1991; Palacky et al., 1981). Four-layer geoelectric model was used to interpret the sounding curves; however, a few of the sounding curves were interpreted with three-layer model. Some of the model resistivity sounding curves obtained are presented in Figure 3. Both the smoothness constrained and robust inversion of the 2D ERI produced useful resistivity anomalies that depict the same geologic features. The 2D resistivity distribution (Figure 4) shows lithologic trend similar to that delineated from the sounding curves.

The geoelectric layers delineated correspond to the collapsed zone, saprolite, saprock and fresh basement. The collapsed zone is composed of lateritic clay characterised by moderately high resistivity anomaly $(70 - 150\Omega m)$. The saprolite which forms the main aquifer unit is characterised with low resistivity anomaly $(1 - 75\Omega m)$; the upper unit of the saprolite is essentially composed of saturated muddy clay while the lower unit is more consolidated and less clayey. The model resistivity of the saprock is significantly higher than that of the regolith but lower than that of the fresh basement which is greater than $2000\Omega m$. Considerable lateral variations in the resistivity model representing variations in thickness and degree of compaction are observed for the collapsed zone and saprolite. Resistivity anomalies representing fractures, vertical contacts, zones of intense weathering, and zones resistant to weathering were delineated on the 2D ERI. The effective porosity and permeability of the weathered and fractured zones are usually higher than the primary porosity and permeability of the basement rocks (McDowell 1979; Olorunfemi et al., 1986). The thickness of the aquifer unit generally increases towards the streams draining the study area with decreasing depth-to-water table from a maximum of about 10.0 m to a minimum of about 1.0 m. Most of the dug wells extract groundwater from the upper saprolite which is clayey and muddy; groundwater extracted from this unit is generally of poor quality and muddy. Groundwater of better quality can be extracted if the wells and/or boreholes are dug or drilled deeper into the less clay lower saprolite.

Conclusions

The lithologic layers delineated in this study include the collapsed zone, saprolite, saprock and fresh basement; other basement features delineated include fractures and vertical contacts, zones of intense weathering, and zones resistant to weathering. The regolith thickness is generally greater than 20 m and up to 60 m in some part of the study area; this regolith thickness can support sufficient drawdown and thus, has the potential for moderate to high groundwater storativity and yield. Boreholes in the study area should be drilled into the regolith as deep as its thickness permit to allow for sufficient drawdown; in areas where the regolith thickness is less than 20 m, the boreholes should be drilled into the saprock as deep as possible. The fractures together with the zones of intense weathering are zones of preferential accumulation of groundwater and thus, should be preferential targets in siting wells and boreholes. This study shows the effectiveness of dipole-dipole array for near-surface characterisation in crystalline basement terrains as the array proved to be particularly useful in detecting weathered and fractured zones. The integration of 2D ERI with VES enhanced the reliability of the characterization. The plaque of electrical equivalence, non-uniqueness and anisotropy that usually leads to ambiguities in the interpretation of sounding curves is minimised since the 2D resistivity images are less affected by these plaques.

Acknowledgements

The authors would like to sincerely thank Messrs F. U. Salifu, D. Aluko, O. Adegbuyiro, K. Ojo, O. Olabiyi and A. Kolawole, who helped with field data collections.

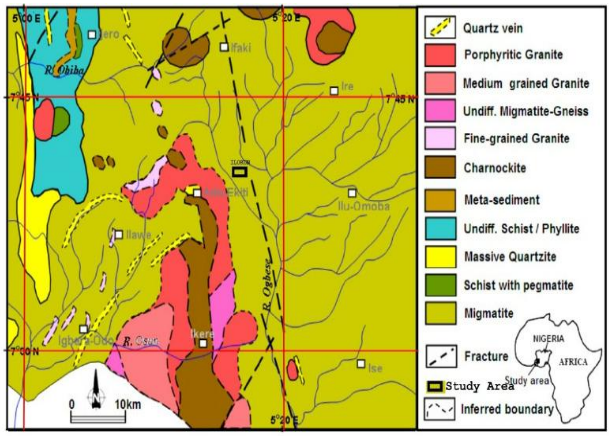

Figure 1: Geological map of Ado-Ekiti and environs

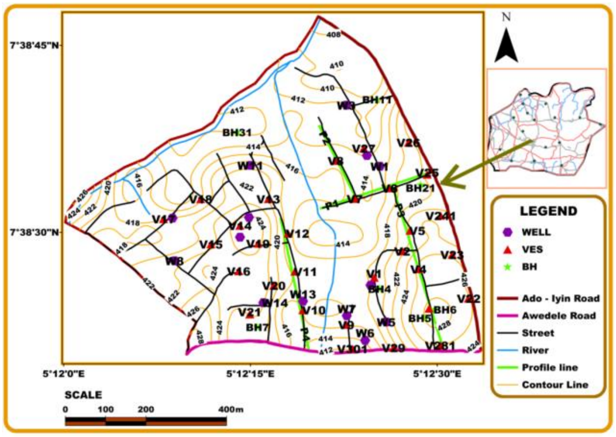

Figure 2: Base map of the study area showing the topography, VES points and 2D traverses

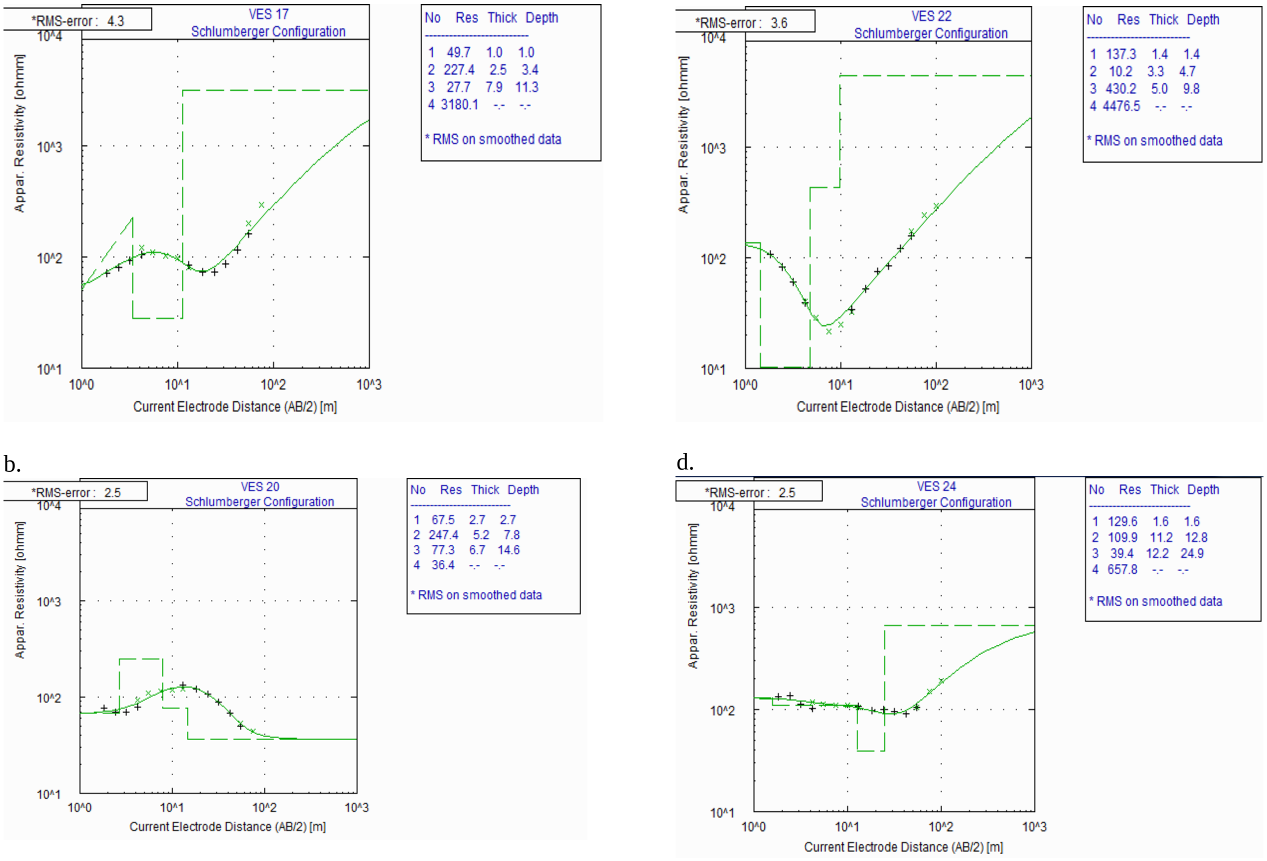
a.

No	Res	Thick	Depth
1	49.7	1.0	1.0
2	227.4	2.5	3.4
3	27.7	7.9	11.3
4	3180.1	-.-	-.-

* RMS on smoothed data

b.

No	Res	Thick	Depth
1	67.5	2.7	2.7
2	247.4	5.2	7.8
3	77.3	6.7	14.6
4	36.4	-.-	-.-

* RMS on smoothed data

c.

No	Res	Thick	Depth
1	137.3	1.4	1.4
2	10.2	3.3	4.7
3	430.2	5.0	9.8
4	4476.5	-.-	-.-

* RMS on smoothed data

d.

No	Res	Thick	Depth
1	129.6	1.6	1.6
2	109.9	11.2	12.8
3	39.4	12.2	24.9
4	657.8	-.-	-.-

* RMS on smoothed data

Figure 3: Selected resistivity sounding curves

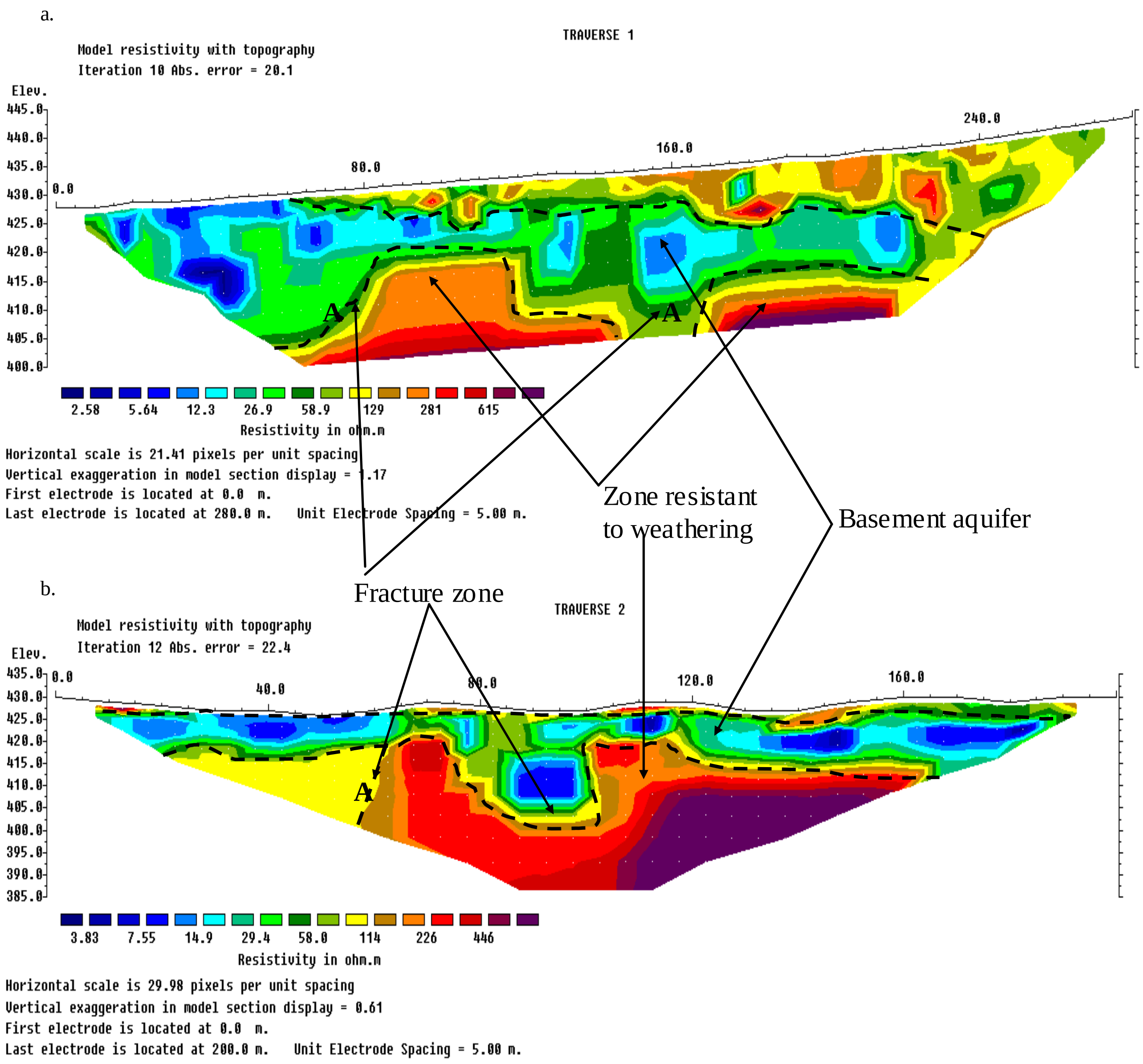

Figure 4: Inverse models of the 2D ERI obtained from the robust inversion constrained for: (a) Traverses 1 and (b) Traverse 2.

Table 1: Survey parameters for 2D ERI

Traverse	**Profile Length (m)**	**Dipole separation (n-factor)**	**Minimum electrode spacing a (m)**	**Maximum Data Levels**
Traverse 1	280	1 - 4	5	6
Traverse 2	200	1 - 4	5	13
Traverse 3	410	1 - 4	10	6
Traverse 4	320	1 - 4	10	4

EDITED REFERENCES

Note: This reference list is a copyedited version of the reference list submitted by the author. Reference lists for the 2017 SEG Technical Program Expanded Abstracts have been copyedited so that references provided with the online metadata for each paper will achieve a high degree of linking to cited sources that appear on the Web.

REFERENCES

Acworth, R. I., 1987, The development of crystalline basement aquifers in a tropical environment: Quarterly Journal of Engineering Geology, **20**, 265–272, http://doi.org/10.1144/GSL.QJEG.1987.020.04.02.

Aizebeokhai, A. P., A. I. Olayinka, and V. S. Singh, 2010, Application of 2D and 3D geoelectrical resistivity imaging for engineering site investigation in a crystalline basement terrain, Southwestern Nigeria: Environmental Earth Sciences, **61**, 1481–1492, http://doi.org/10.1007/s12665-010-0464-z.

Aizebeokhai, A. P., K. D. Oyeyemi, and E. S. Joel, 2016, Groundwater potential assessment in a sedimentary terrain, southwestern Nigeria: Arabian Journal of Geosciences, **9**, 496, http://doi.org/10.1007/s12517-016-2524-5.

Carruthers, R. M., 1985, Review of geophysical techniques for groundwater exploration in crystalline basement terrain. British Geological Survey, Report No. RGRG 85/3, 26p.

Dahlin, T., and Zhou, B., 2004, A numerical comparison of 2D resistivity imaging with ten electrode arrays: Geophysical Prospecting, **52**, 379–398, http://doi.org/10.1111/j.1365-2478.2004.00423.x.

Griffiths, D. H., and R. D. Barker, 1993, Two dimensional resistivity imaging and modelling in areas of complex geology: Journal of Applied Geophysics, **29**, 211–226, http://doi.org/10.1016/0926-9851(93)90005-J.

Kazakis, N., G. Vargemezis, and K. S. Voudouris, 2016, Estimation of hydraulic parameters in a complex porous aquifer system using geoelectrical methods: Science of the Total Environment, **550**, 742–750, http://doi.org/10.1016/j.scitotenv.2016.01.133.

Loke, M. H., 2008, RES2DINV-Rapid 2D resistivity and IP inversion using the least squares method, Geoelectrical imaging 2D and 3D GEOTOMO software, Malaysia, 145pp.

Loke, M. H., and R. D. Barker, 1996, Practical techniques for 3D resistivity surveys and data inversion: Geophysical Prospecting, **44**, 499–524, http://doi.org/10.1111/j.1365-2478.1996.tb00162.x.

Loke, M. H., J. E. Chambers, D. F. Rucker, O. Kuras, and P. B. Wilkinson, 2013, Recent developments in the direct-current geoelectrical imaging method: Journal of Applied Geophysics, **95**,135–156, http://doi.org/10.1016/j.jappgeo.2013.02.017.

McDowell, P. W., 1979, Geophysical mapping of water-filled fracture zones in rocks: Bulletin of the International Association of Engineering Geologists, **19**, 258–264, http://doi.org/10.1007/BF02600485.

Niwas, S., and M. Celik, 2012, Equation estimation of porosity and hydraulic conductivity of Ruhrtal aquifer in Germany using near surface geophysics: Journal of Applied Geophysics, **84**, 77–85, http://doi.org/10.1016/j.jappgeo.2012.06.001.

Olayinka, A. I., 1992, Geophysical siting of boreholes in crystalline basement areas of Africa: Journal of African Earth Science, **14**, 197–207, http://doi.org/10.1016/0899-5362(92)90097-V.

Olayinka, A. I., and U. Yaramanci, 2000, Assessment of the reliability of 2D inversion of apparent resistivity data: Geophysical Prospecting, **48**, 293–316, http://doi.org/10.1046/j.1365-2478.2000.00173.x.

Olurunfemi, M. O., V. O. Olarewaju, and M. Avci, 1986, Geophysical investigations of a fault zones – Case history from Ile-Ife, southwestern Nigeria: Geophysical Prospecting, **34**, 1277–1284, http://doi.org/10.1111/j.1365-2478.1986.tb00528.x.

Palacky, C. J., I. L. Ritsema, and S. J. De Jong, 1981, Electromagnetic prospecting for groundwater in Precambrian terrains in the Republic of Upper Volta: Geophysical Prospecting, **29**, 932–955, http://doi.org/10.1111/j.1365-2478.1981.tb01036.x.

Pous, J., P. Queralt, and R. Chavez, 1996, Lateral and topographic effects in geo-electric soundings: *Journal of Applied Geophysics*, **35**, 237–248, http://doi.org/10.1016/0926-9851(96)00034-1.

Reiser, F., E. Dalsegg, T. Dahlin, G. Ganerod, and J. S. Ronning, 2009, Resistivity modelling of fracture zones and horizontal layers in Bedrock. NGU Report 2009.070, 1–120.

Rucker, D., M. H. Loke, M. T. Levith, and G. E. Noonan, 2010, Electrical resistivity characterization of an industrial site using long electrodes: Geophysics, **75**, no. 4, WA95–WA104, https://doi.org/10.1190/1.3464806.

Wiwattanachang, N., and P. H. Giao, 2011, Monitoring crack development in fibre concrete beam by using electrical resistivity imaging: Journal of Applied Geophysics, **75**, no. 2, 294–304, https://doi.org/10.1016/j.jappgeo.2011.06.009.

Wright, E. P., 1992, The hydrogeology of crystalline basement aquifers in Africa, *in* E. P. Wright, and W. G. Burgess, eds., Hydrogeology of crystalline basement aquifers in Africa: Geological Society Special Publications **66**, 1–27.